DOI: 10.1021/ma900847r

Macromolecules
ARTICLE

Synthesis, Electronic, and Emission Spectroscopy, and Electrochromic Characterization of Azulene−Fluorene Conjugated Oligomers and Polymers

Xiaobai Wang,[†,§] Joseph Kok-Peng Ng,[†,§] Pengtao Jia,[†,‡,§] Tingting Lin,[†] Ching Mui Cho,[†] Jianwei Xu,*[,†] Xuehong Lu,[‡] and Chaobin He[†]

[†]*Institute of Materials Research and Engineering, A*STAR (Agency for Science, Technology and Research), 3 Research Link, Singapore 117602, Republic of Singapore, and* [‡]*School of Materials Science and Engineering, Nanyang Technological University, 50 Nanyang Avenue, Singapore 639798, Republic of Singapore.* [§] *These authors made equal contributions to this paper.*

Received April 17, 2009; Revised Manuscript Received June 4, 2009

ABSTRACT: Two model compounds, 1,3-bis(9,9-dihexylfluoren-2-yl)azulene (**M1**), and 1,3-bis[7-(9,9,-9′,9′-tetrahexyl-2,2′-bifluoren-7-yl)azulene (**M2**), and polymers, poly[2,7-(9,9-dialkylfluorenyl)-*alt*-(1′,3′-azulenyl)] **(P1−P4)** and poly{[1,3-bis(9′,9′-dihexylfluoren-2′-yl)azulenyl]-*alt*-[2″,7″-(9″,9″-dialkylfluorenyl]} (**P5**, **P6**) were synthesized by reacting 1,3-dibromoazulene or 1,3-bis(7-bromo-9,9-dihexylfluoren-2-yl) azulene with a suitable 9,9-dialkylflourenyl-2-borate or 2,7-diborate via Suzuki cross-coupling reactions. The thermal and optical properties of the polymers were characterized by thermogravimetric analysis, differential scanning calorimetry, and UV−vis and fluorescence spectroscopy. **M1**, **M2**, and **P1−P6** are nonfluorescent in the neutral state in different organic solvents. However, **M1**, **M2**, **P5**, and **P6** become fluorescent upon the addition of trifluoroacetic acid in THF, with relative quantum efficiencies of 0.004−0.06. The "switching on" of the fluorescence for the azulene−fluorene copolymers and model compounds is due to the formation of a 6π electron aromatic azulenium cation, which alters the overall electronic character, particularly, the HOMO and LUMO, and subsequently the band gap. Cyclic voltammograms of polymer films prepared by spin-coating polymer solution onto an indium−tin oxide-coated glass substrate showed that all of the polymers films exhibited the relatively low half-wave oxidation potentials in the range 0.84−0.93 V vs Ag/AgCl. Electrochromic devices of **P3** and **P5** with a sandwich structure of PET-ITO/polymer/PMMA-PC-$LiClO_4$/PET-ITO were fabricated, and color changes from light yellow to brown and from yellow to green for polymers **P3** and **P5** films, respectively, are observed.

Introduction

1wAs nonalternant aromatic hydrocarbons, azulene and its derivatives have been the subject of many experimental and theoretical studies during the past a few decades[1−11] due to their unusual electronic character and anomalous spectral behaviors, including the formation of a dipolar structure with a dipole moment of around 1.0 D and unusual S_2-S_0 fluorescence. Azulene has received much attention in various areas of molecular materials research, such as liquid crystals,[12,13] conducting polymers,[14−16] optoelectronic molecular switches,[17] anion receptors,[18−20] and nonlinear optical (NLO) material.[21,22] Recently, developments of homo- and copolymers containing the azulene motif have been explored. For example, poly(azulene) prepared from azulene in warm or hot trifluoroacetic acid (TFA) was first reported by Kihara[23] in 1997. A few years later, Lai's group reported a new method to synthesize high molecular-weight poly(1,3-azulene) with electrical conductivities of 0.74−1.22 S cm^{-1} through the polymerization of 1,3-dibromozaulene in the presence of catalytic amounts of Ni(COD)$_2$.[24] The same research group subsequently reported a series of highly conductive azulene−thiophene conjugated polymers.[13,14,25]

*To whom correspondence should be addressed. E-mail address: jw-xu@imre.a-star.edu.sg. Telephone: (65)-6872-7543. Fax: (65)-6872-7528.

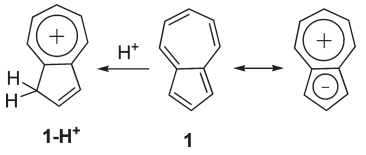

In contrast to other fused aromatic compounds, azulene shows the anomalous fluorescence from the S_2 state and only extremely weak S_1-S_0 fluorescence with an exceptionally low quantum efficiency of $\sim 10^{-6}$ and a very short lifetime of 7.5 ps.[26] This is because the particularly low lying excited state, S_1, and the large S_1-S_2 energy gap, as well as the presence of a fast radiationless relaxation from the S_1 state to the ground state (less 1 ps), leads to the extremely weak S_1-S_0 fluorescence.[27] In theory, azulene can be considered an aromatic 6π electron tropylium cation fused by a 6π electron cyclopentadienyl anion. The electron-rich cyclopentadienyl anion allows azulene to easily undergo electrophilic substitution at C-1 or C-3 in the 5-membered ring to form a very stable aromatic 6π-electron azulenium ion, which can be considered as a vinyl-substituted tropylium cation. The formation of the tropylium structure in several azulene derivatives has been reported to result in interesting electrochemical behaviors[28,29] and electrochromism.[30,31] Therefore, this facile chemical transformation of protonating azulene units to form an azulenium structure in the azulene-containing polymers could be employed

 Published on Web 06/24/2009

to tune or even alter the overall physical properties of the polymers, e.g., "switching on" of the fluorescence, or alteration of electrical conductivity, etc. On the other hand, azulene readily loses one electron during oxidation to give a radical azulenium cation in which the cationic part exists as a stabilized aromatic tropylium ion. Azulene has a relatively low oxidation potential and is more easily oxidized than most common aromatic carbocycles and heterocycles.[32] For example, its oxidation potential (0.96 V vs. SCE[32] (saturated calomel electrode)) is lower than that of the 10π-electron fused aromatics naphthalene with the same molecular formula of $C_{10}H_8$ (1.64 V vs. SCE[33,34]). Thus azulene-containing polymers are expected to easily undergo a redox reaction at the azulene unit to form an azulenium radical cation, and could potentially function as a new class of electrochromic material.

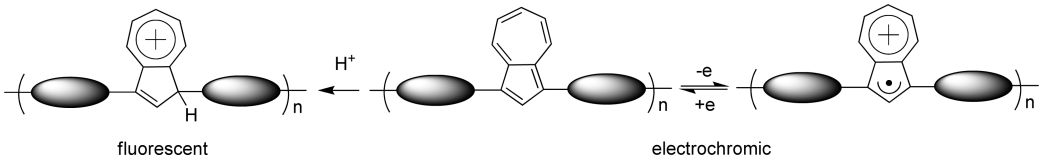

Herein we report the synthesis of 1,3-difluorenyl substituted azulenes and fluorene-azulene conjugated copolymers via a Suzuki cross-coupling reaction using $Pd(PPh_3)_4$ as catalyst. The studies show that 1,3-bis(9,9-dihexylfluoren-2-yl)azulene (**M1**), 1,3-bis[7-(9,9,9′,9′-tetrahexyl-2,2′-bifluoren-7-yl)azulene (**M2**), poly-[2,7-(9,9-dialkyllfluorenyl)-*alt*-(1′,3′-azulenyl)] (**P1**−**P4**) and poly-{[1,3-bis(9′,9′-dihexylfluoren-2′-yl)azulenyl]-*alt*-[2″,7″-(9″,9″-dialkyl-fluorenyl]} (**P5**, **P6**) are nonfluorescent in organic solvents in the neutral state, but the addition of trifluoroacetic acid (TFA) to polymers **P5**, **P6** and model compounds **M1**, **M2** in THF leads to "switching on" of fluorescence. Polymer films of **P1**−**P6** also exhibited electrochromic properties, and their corresponding electrochromic devices were fabricated. To the best of our knowledge, this paper illustrates the first example of azulene-containing conjugated polymers being used as electrochromic materials.

Experimental Section

Materials. Azulene and 9,9-dialkylfluorene 2,7-bis(trimethyleneborate)s were purchased from Aldrich and purified by crystallization before use. 1,3-Dibromoazulene (**2**) was synthesized according to the literature.[39] Other commercially available reagents and solvents were used as received.

Instrumentation. ^{1}H and ^{13}C nuclear magnetic resonance (NMR) spectra were recorded on a Bruker DRX 400-MHz NMR spectrometer in $CDCl_3$ at room temperature using tetramethylsilane (TMS) as an internal standard. Operating frequencies of the NMR spectrometer were 400.13 MHz (^{1}H) and 100.61 MHz (^{13}C). Electron impact mass spectra (EIMS) and high resolution MS (HRMS) were recorded using a Micromass 7034E mass spectrometer. Elemental analysis was conducted on a Perkin-Elmer 240C elemental analyzer for C, H, and N determination. Thermal analysis was performed in a Perkin-Elmer thermogravimetric analyzer (TGA 7) in nitrogen or in air at a heating rate of 20 °C min^{-1} and on a TA Instruments Differential Scanning Calorimetry (DSC) 2920 at a heating rate and a cooling rate of 5 °C min^{-1}in nitrogen. Gel permeation chromatography (GPC) analyses were carried out on a Waters 2690 system using polystyrene as standards and THF as eluent. UV−vis and fluorescence spectra were obtained using a Shimadzu UV3101PC UV−vis-NIR spectrophotometer and a Perkin-Elmer LS 50B luminescence spectrometer with a Xenon lamp as light source, respectively. The fluorescence quantum efficiencies (ϕ_f) of the polymers in THF solutions were measured by using quinine sulfate (1×10^{-5} M solution in 0.1 M H_2SO_4, assuming $\phi_f = 0.55$) as a standard.

Cyclic Voltammograms and Device Fabrication. The solutions of polymers in xylene were spin-coated onto indium tin oxide (ITO) electrodes laminated on poly(ethylene terephthalate) (PET) substrates (100 Ω/sq) to form electrochromic layers. The gel electrolyte was prepared by mixing poly(methacrylate) (PMMA, $M_w = 120\,000$ g/mol), $LiClO_4$ and propylene carbonate (PC) in dry acetonitrile according to the literature.[35−38] Electrochromic devices with a sandwich structure of PET-ITO/electrochromic polymer/gel polyelectrolyte//PET-ITO were then fabricated. The in situ spectro-electrochemical properties of the devices were characterized using an Autolab PGSTAT30 electrochemical workstation and a Shimadzu 5301 UV−vis spectrophotometer. The CV experiments were carried out in a three-electrode arrangement using two PET/ITO (100Ω/sq) electrodes and Ag/AgCl (3 M KCl) as the reference electrode.

Calculation Method. The HOMO and LUMO of **M1** and **M2** were estimated using the density functional theory electronic structure program DMol^3 available as part of Materials Studio (Accelrys Inc.). In this code, the electronic wave function was expanded in a localized atom-centered basis set with each basis function defined numerically on a dense radial grid. All-electron calculations were performed with a double numeric polarized (DNP) basis set (which is analogous to the Gaussian 6-31(d,p) basis set), the most complete set available in the code. The gradient-corrected PW91 functional, a finite basis-set cutoff of 3.7 Å and a "fine" quality (convergence tolerances, energy 1.0×10^{-5} Ha, maximum force 0.002 Ha Å^{-1}; maximum displacement 0.005 Å; SCF tolerance 1.0×10^{-6}) were used.

Synthesis of Compounds and Polymers. *2-(4,4,5,5-Tetramethyl-1,3,2-dioxaboralan-2-yl)-9,9-dihexylfluorene (3).* Compound **3** was synthesized by reacting 2-bromofluorene with 1-bromohexane, followed by boronation using 2-isopropoxy-4,4,5,5-tetramethyl-1,3,2-dioxaborolane. 2-Bromo-9,9-dihexylfluorene: An aqueous solution of NaOH (50%, 80 mL) was directly added to a DMSO suspension (333 mL) of 2-bromofluorene (50.0 g, 204 mmol) containing Aliquot 336 (0.82 g, 2.01 mmol) as a phase transfer catalyst. 1-Bromohexane (84.2 g, 510 mmol) was added to the above mixture with stirring. The reaction mixture was stirred vigorously at room temperature with the protection of argon for 4 days. Ethyl acetate (500 mL) was then added to the mixture and the precipitated NaBr was filtered off. The filtrate was concentrated to a volume of *ca*. 300 mL to which 1 M HCl (1 L) was added. The color of the organic layer was changed from bluish-green to an orange-yellow. The organic layer was separated and dried over anhydrous $MgSO_4$. The concentrated crude orange oil was purified by chromatography on silica gel using hexane to afford the desired product as a yellow oil (81.7 g, yield, 96%).^{1}H NMR: δ 7.67 (m, 1H), 7.55 (d, 1H, $J = 8.0$ Hz), 7.44−7.46 (m, 2H), 7.32 (m, 3H), 1.89−1.98 (m, 4H), 1.03−1.14 (m, 12H), 0.77 (t, 6H, $J =$ 7.2 Hz), 0.60 (m, 4H). ^{13}C NMR: δ 153.4, 150.7, 140.6, 140.5, 130.3, 127.8, 127.3, 126.6, 123.3, 121.4, 120.1, 55.8, 40.7, 31.8, 30.0, 24.1, 22.9, 14.3.

2-Bromo-9,9-dihexylfluorene (20.0 g, 48.3 mmol) was added into freshly distilled THF (150 mL). The mixture was purged with N_2 and cooled to −78 °C. *n*-BuLi (55.76 mL, 72.49 mmol) was added via syringe. The reaction was allowed to stir at 0 °C

for 30 min and was then chilled to − 78 °C again. 2-Isopropoxy-4,4,5,5-tetramethyl-1,3,2-dioxaborolane (10.8 g, 58.0 mmol) was syringed rapidly into the solution, and the reaction was continued for another 1 h. After that the mixture was stirred for 16 h at room temperature. The reaction mixture was then poured into water and extracted with diethyl ether. The extracts were dried over anhydrous $MgSO_4$. The crude product was purified by chromatography on silica gel using hexane followed by hexane: ethyl acetate (10:1 v/v). The final product was obtained as a viscous oil (12.9 g, yield, 57.8%). ^{1}H NMR: δ 7.79 (m, 1H), 7.70−7.42 (m, 3H), 7.32 (m, 3H), 1.97 (m, 4 H), 1.39 (s, 12H), 1.02−1.10 (m, 12H), 0.75 (t, 6 H, J = 7.0 Hz), 0.58 (br, s, 4H). ^{13}C NMR: δ 151.7, 150.3, 144.5, 141.4, 134.1, 129.3, 127.8, 127.1, 123.3, 120.5, 119.3, 84.1, 55.5, 40.6, 31.8, 30.1, 25.3, 24.1, 22.9, 14.3.

1,3-Bis(9,9-dihexylfluoren-2-yl)azulene (M1). To a degassed toluene solution (70 mL) of **2** (0.73 g, 2.54 mmol) were added **3** (5.84 g, 12.7 mmol), $Pd(PPh_3)_4$ (0.162 g, 0.141 mmol) and Aliquot 336 (1 mL). A degassed aqueous solution of Na_2CO_3 (10.8 g, 50 mL) was added next. The mixture was refluxed at 103 °C for 20 h. After cooling, the organic layer was separated, concentrated, and redissolved in CH_2Cl_2 (30 mL). This solution was washed twice with brine (20 mL). The combined organic extracts were dried over anhydrous $MgSO_4$. The crude product was purified by chromatography on silica gel using hexane. A green flaky solid (1.65 g) was obtained after evaporation and was dried in a vacuum oven (yield, 82.0%). ^{1}H NMR: δ 8.61 (d, 2H, J = 9.9 Hz), 8.29 (s, 1H), 7.86 (d, 2H, J = 7.0 Hz), 7.78 (d, 2H, J = 7.3 Hz), 7.59−7.65 (m, 4H), 7.61 (t, 1H, J = 9.6 Hz), 7.32−7.41 (m, 6H), 7.13 (t, 2H, J = 6.5 Hz), 2.04−2.07 (m, 8H), 1.18−1.19 (m, 24H), 0.78−0.81 (m, 20H). HRMS (EI): calcd for $C_{60}H_{72}$, m/z 793.2364; found, m/z 793.3529. Anal. Calcd for $C_{60}H_{72}$: C, 90.85; H, 9.15. Found: C, 90.74; H, 9.34.

1,3-Bis(7-bromo-9,9-dihexylfluoren-2-yl)azulene (4). To a benzene solution (50 mL) were added **3** (1.59 g, 2.00 mmol) and NBS (0.856 g, 4.81 mmol) directly. The mixture was stirred at room temperature for 2.5 h. The mixture was washed with water (2 × 50 mL), and then the organic phase was separated and concentrated. The crude compound was purified by chromatography on silica gel using hexane/chloroform as eluents (gradually increasing eluent polarities from 1:0, to 10:1, 5:1, and finally 4:1 v/v). A brown flaky solid (1.84 g, 1.90 mmol) was obtained after drying in vacuum oven (yield, 95.2%). ^{1}H NMR: δ 8.66 (d, 2H, J = 1.9 Hz), 8.31 (s, 1H), 8.19 (m, 1H), 7.86 (d, 2H, J = 7.6 Hz), 7.77 (d, 2H, J = 7.6 Hz), 7.56−7.60 (m, 4H), 7.32−7.40 (m, 6H), 2.04 (m, 8H), 1.05−1.29 (m, 24H), 0.70−0.78 (m, 20H). ^{13}C NMR: δ 151.9, 151.4, 143.7, 141.2, 140.9, 140.8, 138.9, 135.1, 134.7, 133.1, 129.0, 127.6, 127.3, 124.5, 123.4, 120.6, 120.2, 116.9, 55.6, 40.9, 31.9, 30.2, 24.3, 23.0, 14.3. HRMS (EI): calcd for $C_{60}H_{70}Br_2$, m/z 951.0276; found, m/z 950.2519. Anal. Calcd for $C_{60}H_{70}Br_2$: C, 75.78; H, 7.42. Found: C, 75.75; H, 7.88.

1,3-Bis[7-(9,9,9′,9′-tetrahexyl-2,2′-bifluoren-7-yl)azulene (M2). To a degassed toluene (35 mL) solution of **M1** (2.09 g, 6.32 mmol) were added **4** (1.20 g, 1.26 mmol) and $Pd(PPh_3)_4$ (0.0810 g, 0.0701 mmol), followed by a degassed aqueous solution of Na_2CO_3 (5.36 g, 25.3 mL). A few drops of Aliquot 336 were then added. The mixture was refluxed at 103 °C for 16 h under an atmosphere of N_2. The organic layer was separated after the reaction and washed with brine (2 × 100 mL). The remaining aqueous solution was extracted with CH_2Cl_2 (3 × 50 mL), and the organic layers were combined together, dried over anhydrous $MgSO_4$, and concentrated. The crude product was purified by chromatography on silica gel using $CHCl_3$/hexane (from 0:1 to 1:1 v/v). The deep green product was obtained after drying in a vacuum oven (yield, 70.0%). ^{1}H NMR: δ 9.01 (s, 2H), 8.31 (s, 1H), 8.26 (s, 1H), 7.84 (d, 2H, J = 7.6 Hz), 7.63−7.78 (m, 14H), 7.28−7.36 (m, 12H), 2.01 (m, 16H), 0.90−1.15 (m, 48H), 0.62−0.78 (m, 40H). ^{13}C NMR: δ 152.1, 151.4, 151.3, 144.9, 141.4, 141.0, 140.6, 140.2, 139.5, 138.5, 137.8, 137.2, 137.0, 136.5, 136.1, 132.7, 128.8, 127.5, 127.2, 124.6, 123.4, 123.0, 120.4, 120.2, 120.1, 55.6, 40.9, 40.8, 31.9, 30.2, 24.3, 23.0, 14.4. MS (EI): m/z 1458.0 (M^+). Anal. Calcd for $C_{110}H_{136}$: C, 90.60; H, 9.40. Found: C, 90.75; H, 9.67.

Synthesis of Polymer. *General Synthetic Procedures for Polymers P1−P6*. To a dissolved mixture of **2** or **4** (1.64 mmol), 9,9-dialkylfluorene-2,7-bis(trimethyleneborate) (1.64 mmol) and $Pd(PPh_3)_4$ (0.019 g, 0.0164 mmol) in dry toluene (25 mL) were added, followed by a degassed aqueous solution (17 mL) of Na_2CO_3 (3.60 g, 34.0 mmol). The mixture was stirred and refluxed under N_2 at 123 °C for 4 days. The mixture was then poured into excess methanol (250−300 mL) with vigorous stirring. The obtained precipitate was filtered, washed with water, and dried under vacuum. The crude product was dissolved in $CHCl_3$ and filtered. The green filtrate was evaporated to dryness, and was dissolved in a minimum volume of toluene. Sufficient methanol was then added to reprecipitate the product. The green precipitate was finally washed with acetone using a Soxhlet extractor for 2 days. The final product was obtained after drying in a vacuum oven at 60 °C for 2 days.

Poly[2,7-(9,9-dihexylfluorenyl)-alt-(1′,3′-azulenyl)] (P1). Yield: 79.2% (0.597 g, 1.30 mmol). ^{1}H NMR: δ 8.63 (m, 2H), 8.30−8.38 (m, 1H), 7.37−7.91 (m, 7H), 7.13−7.16 (m, 2H), 2.11 (m, 4H), 0.78−1.16 (br, m, 22H). ^{13}C NMR: δ 151.9, 140.0, 139.5, 138.1, 137.7, 137.4, 136.8, 131.8, 129.2, 124.8, 123.8, 120.3, 55.7, 40.9, 32.0, 30.2, 24.5, 23.0, 14.4. Anal. Calcd for $(C_{35}H_{38})_n$: C, 91.65; H, 8.35. Found: C, 91.17; H, 8.50

Poly[2,7-(9,9-dioctylfluorenyl)-alt-(1′,3′-azulenyl)] (P2). Yield: 75.7%. ^{1}H NMR: δ 8.65 (m, 2H), 8.34 (s, 1H), 7.63−7.94 (m, 7H), 7.14−7.18 (m, 2H), 2.13 (br, m, 4H), 0.79−1.17 (m, 30H). ^{13}C NMR: δ 151.9, 140.0, 139.4, 137.6, 137.4, 136.7, 136.2, 131.8, 129.2, 124.9, 123.8, 120.3, 55.7, 40.9, 32.2, 30.6, 29.7, 29.6, 24.6, 23.0, 14.3. Anal. Calcd for $(C_{39}H_{46})_n$: C, 90.99; H, 9.01. Found: C, 90.41; H, 9.47.

Poly[2,7-(9,9-didodecylfluorenyl)-alt-(1′,3′-azulenyl)] (P3). Yield: 89.2%. ^{1}H NMR: δ 8.64 (m, 2H), 8.34 (m, 1H), 7.62−7.93 (m, 7H), 7.14 (m, 2H), 2.11 (m, 4H), 0.83−1.18 (m, 46H). ^{13}C NMR: δ 152.0, 140.0, 139.5, 137.6, 137.4, 136.8, 136.2, 131.8, 129.2, 124.8, 123.8, 120.3, 55.7, 41.0, 32.3, 30.6, 30.0, 29.8, 29.7, 24.6, 23.1, 14.5. Anal. Calcd for $(C_{47}H_{62})_n$: C, 90.03; H, 9.97. Found: C, 89.57; H, 10.38.

Poly[2,7-(9,9-di(2′-ethylhexyl)fluorenyl)-alt-(1″,3″-azulenyl)] (P4). Yield: 82.4%. ^{1}H NMR: δ 8.62 (m, 2H), 8.20 (m, 1H), 7.10−7.90 (m, 9H), 2.12 (m, 4H), 0.56−0.95 (m, 30H). ^{13}C NMR: δ 151.6, 140.3, 139.3, 137.7, 137.3, 136.7, 132.0, 129.2, 126.0, 123.5, 120.2, 55.6, 45.5, 35.3, 35.2, 34.4, 28.7, 27.5, 23.3, 14.4, 10.8. Anal. Calcd for $(C_{39}H_{46})_n$: C, 90.99; H, 9.01. Found: C, 90.50; H, 9.45.

Poly{[1,3-bis(9′,9′-dihexylfluoren-2′-yl)azulenyl]-alt-[2″,7″-(9″,9″-dihexylfluorenyl]} (P5). Yield: 67.0%. ^{1}H NMR: δ 9.05 (m, 2H), 8.32 (m, 2H), 7.67−7.87 (m, 15H), 7.33−7.37 (m, 5H), 2.05 (m, 12H), 0.64−1.06 (m, 66H). ^{13}C NMR: δ 152.4, 152.1, 151.3, 145.1, 141.4, 140.2, 140.1, 137.1, 136.5, 136.1, 132.8, 128.7, 127.2, 124.7, 123.3, 120.6, 120.1, 55.8, 55.6, 40.9, 31.9, 30.2, 24.3, 22.9, 14.3. Anal. Calcd for $(C_{85}H_{102})_n$: C, 90.85; H, 9.15. Found: C, 90.45; H, 9.60.

Poly{[1,3-bis(9′,9′-dihexylfluoren-2′-yl)azulenyl]-alt-[2″,7″-(9″,9″-didodecyl)fluorenyl]} (P6). Yield: 59.1%. ^{1}H NMR: δ δ 9.05 (m, 2H), 8.30 (m, 2H), 7.68−7.90 (m, 15H), 7.20−7.38 (m, 5H), 2.03 (m, 12H), 0.90−1.28 (m, 60H), 0.64 − 0.85 (m, 30H). ^{13}C NMR: δ 152.4, 152.1, 151.7, 151.3, 145.0, 144.4, 141.4, 140.2, 139.4, 138.6, 137.0, 136.5, 136.1, 132.8, 128.7, 127.2, 124.7, 123.3, 120.6, 120.1, 55.8, 55.6, 40.9, 32.3, 31.9, 30.6, 30.0, 29.7, 24.6, 24.2, 23.0, 22.9, 14.4, 14.3. Anal. Calcd for $(C_{97}H_{126})_n$: C, 90.17; H, 9.83. Found: C, 89.74; H, 10.07.

Results and Discussion

Synthesis and Characterization of Model Compounds and Polymers. The synthetic routes leading to model compounds **M1** and **M2** and polymers **P1-−P6** are shown in Schemes 1 and 2, respectively. First, 1,3-dibromoazulene

Scheme 1. Synthetic Routes Leading to Model Compounds M1 and M2[a]

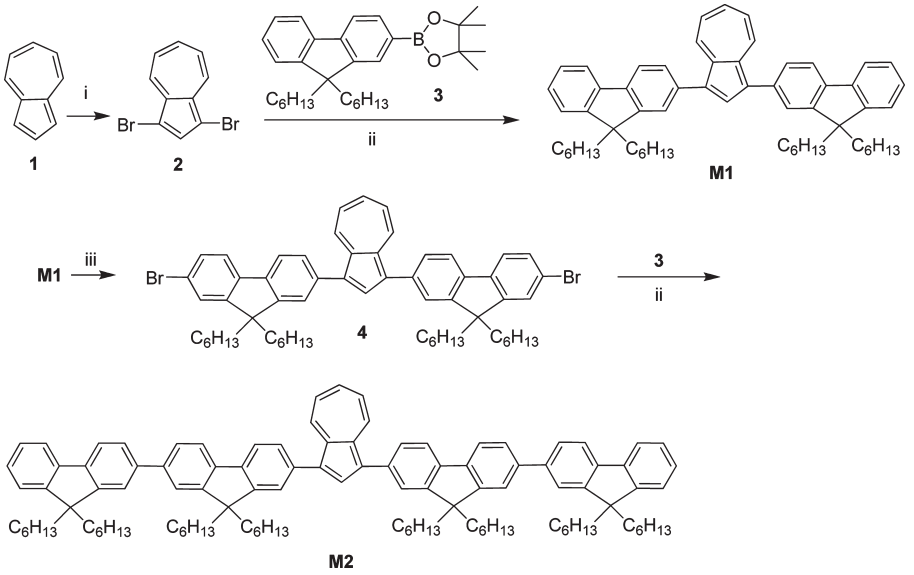

[a] Reaction conditions: (i) NBS, benzene, room temperature (rt); (ii) $Pd(PPh_3)_4$, 2M K_2CO_3, toluene, Aliquat 336, 103°C; (iii) NBS, $CHCl_3$, rt.

Scheme 2. Synthetic routes leading to polymers P1−P6[a]

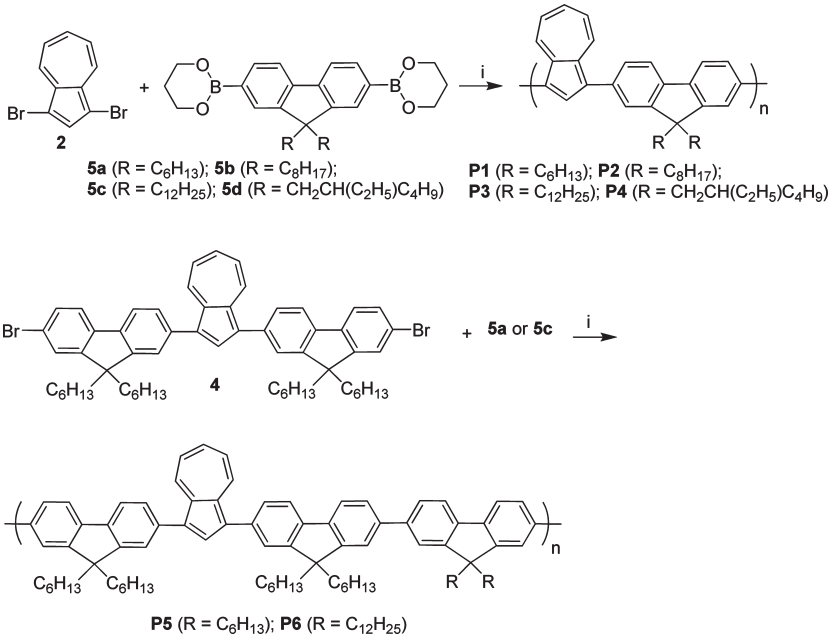

[a] Reaction conditions: (i) $Pd(PPh_3)_4$, 2M K_2CO_3, toluene, Aliquat 336, 123°C.

(**1**) was prepared according to a literature method with modification.[39] 2-(4,4,5,5-Tetramethyl-1,3,2-dioxaboralan-2-yl)-9, 9-dihexylfluorene (**3**) was obtained by reacting 2-bromo-9, 9-dihexylfluorene with 2-isopropoxy-4,4,5,5-tetramethyl-1,3, 2-dioxaborolane in the presence of *n*-BuLi. Compound **M1** was then synthesized in 82% yield by reacting **1** and **3** via a Suzuki cross-coupling reaction using $Pd(PPh_3)_4$ as catalyst. Further bromination of **M1** in benzene using *N*-bromosuccinimide (NBS) afforded dibromide **4** in 95% yield. Similarly, a Suzuki cross-coupling reaction between **3** and **4** gave **M2** in 65% yield. Both **M1** and **M2** were stable even after exposure to air and ambient light at room temperature for a few months. All new compounds synthesized in this paper were characterized by spectroscopic methods and elemental analysis.

The palladium-catalyzed Suzuki polymerization reaction in toluene/2 M K_2CO_3 between **2** or **4** and suitable 9,9-dialkyl-fluorene-2,7-diborates (**5a**−**5d**) afforded polymers **P1**−**P6** in reasonable yields. The polymers were purified by solvent precipitation and Soxhlet extraction with acetone to give dark blue solids. These polymers were found to be soluble in organic solvents such as tetrahydrofuran (THF), dichloromethane, chloroform and toluene. The polymers were structurally characterized by various spectroscopic methods and elemental analysis. As an example, the ^{1}H NMR spectrum of **P5** is illustrated in Figure 1. The presence of signals at δ 9.03, 8.33, and 8.27 with an integration ratio of 2:1:1, which are assigned to protons H4,8, H6, and H2 of azulene, respectively, indicates that the azulene rings remained intact during the reaction and purification process. The molecular weights of these polymers against polystyrene standards were determined by gel permeation chromatography (GPC) and the data are summarized in

Table 1. The polymers have molecular weights of 6800−12500 with a polydispersity of 1.29−2.21. The polymers exhibited high thermal stability with decomposition temperatures ranging from 414 to 447 °C in nitrogen. However, no glass transitions were detected by DSC.

UV−Vis Spectroscopy and Color Change. The UV−visible spectra of model compounds **M1**−**2** in THF and THF/TFA were measured and are shown in Figure 2. Three absorption bands centered at 331 (58 700), 395 (14 400), and 630 (260) nm were observed in the electronic absorption spectra of **M1** in THF (the values in the parentheses are the molar absorptivities with units of L mol^{-1} cm^{-1}). Similarly, **M2** showed two π - π absorption bands at 341 (35 600) and 449 (11 800) nm associated with a long wavelength absorption at 654 (380) nm. The two $\pi-\pi$ absorption bands of **M2** were red-shifted by 10 and 54 nm, respectively, when compared to **M1** due to the longer conjugation length of **M2**. The weak broad bands centered at 630 and 654 nm, respectively, for **M1** and **M2**, correspond to their S_0-S_1 bands.

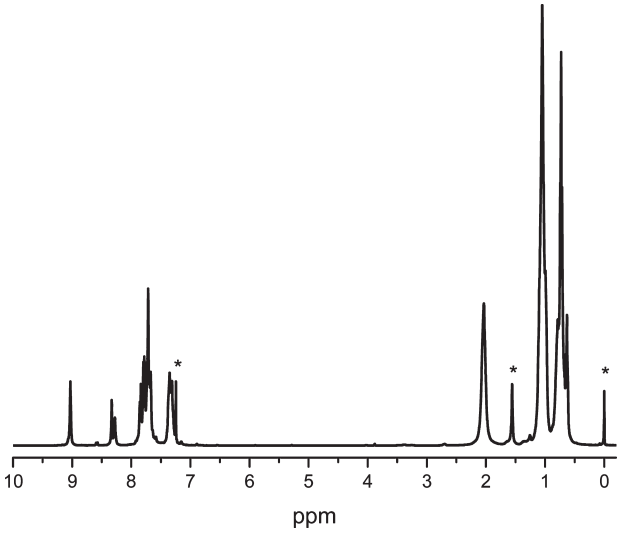

Figure 1. ^{1}H NMR spectrum of polymer **P5** in $CDCl_3$. Asterisks indicate TMS, water, and solvent residual.

Table 1. Synthetic Yields, Molecular Weights, M_w/M_n and Thermal Data of P1-6[a]

polymers	yield (%)	M_w	M_n	M_w/M_n	T_d (in N_2)	T_d (in air)
P1	79.2	17200	9700	1.67	442	433
P2	75.7	25400	12500	2.04	447	434
P3	89.2	21000	9500	2.21	441	426
P4	82.4	9300	6800	1.37	440	419
P5	67.0	15800	8600	1.94	414	408
P6	59.1	17200	10400	1.29	434	414

[a] M_w: the weight-average molecular weight. M_n: the number-average molecular weight. T_d: the decomposition temperature at which 5% weight loss occurs.

Upon the addition of TFA to a solution of **M1** in THF solution, the intensity of the shoulder peak at 395 nm gradually decreased with the increase of the TFA, and finally disappeared when the TFA concentration approached 30%. Meanwhile, the absorption maxima (λ_{max}) of **M1** blue-shifted from 331 to 311 nm, accompanying with the disappearance of the long wavelength absorption band at 630 nm. In contrast, upon the addition of TFA to a solution of **M2** in THF, a new band at 508 nm was observed, which was attributed to the formation of the azulenium cation. An increase in the TFA concentration and a rise in absorbance intensity of the band at 508 nm, along with the decrease of absorbance intensity of the bands at 654 nm, were in accordance with a bleaching of the $\pi-\pi$ transition band at 449 nm. Two isosbestic points were clearly observed at 474 and 629 nm (Figure 2b), suggesting that only two interconverting optically different species (neutral **M2** and **M2**−H^+) were present in the system. Compared to the absorption λ_{max} of the parent azulenium cation ion (**1**−H^+, λ_{max} = 352 nm),[40,41] **M2**−H^+ showed a remarkable red shift of 156 nm due to the attachment of two bisfluorene moieties.

The UV−vis spectra of polymers **P1**−**P4** and **P5** and **P6** are shown in Figures 3 and 4, respectively. The absorption and emission spectroscopic data (see vide infra) are summarized in Table 2. **P1**−**P4** showed similar UV−vis spectral profiles in both the neutral state and in the presence of TFA. For example, **P1** exhibited one strong π - π absorption band at 362 nm and two weak bands at 477 and 630 nm, in which the long wavelength band was assigned to the S_0-S_1 absorption. In contrast, significant changes in the absorption spectrum of polymer **5** or **6** in THF associated with different TFA concentrations were found to follow a similar tend as those observed in UV−vis spectra of **M2** as described above. For instance, neutral **P5** showed two strong absorption bands at 347 and 464 nm and a very weak band at 669 and 772 nm. Upon the

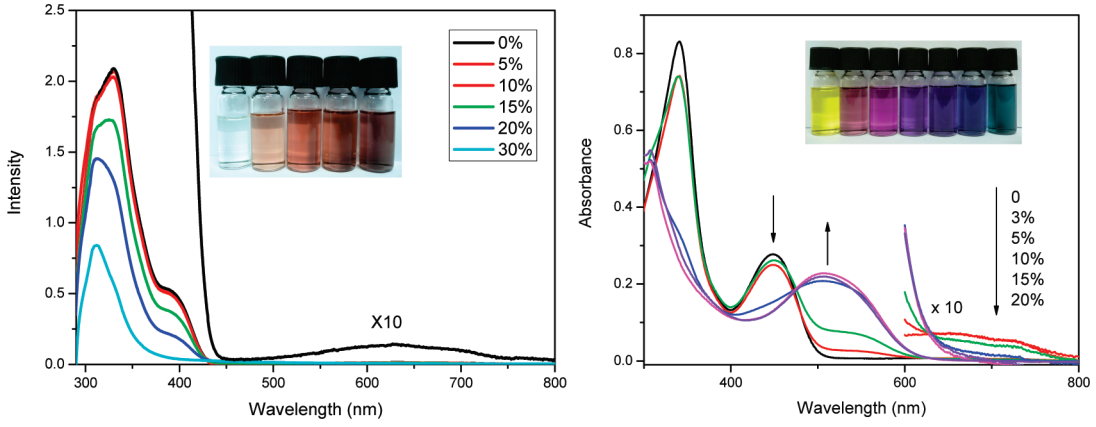

Figure 2. UV−vis spectral and color changes of (a) **M1** (3.53×10^{-5} M) (inset: from left to right, **M1** in 0%, 5%, 10%, 20%, and 30% TFA/THF, v/v), and (b) **M2** (2.34×10^{-5} M) (inset: from left to right, **M2** in 0%, 3%, 5%, 7%, 10%, 15%, and 20% TFA/THF, v/v), upon addition of TFA in THF.

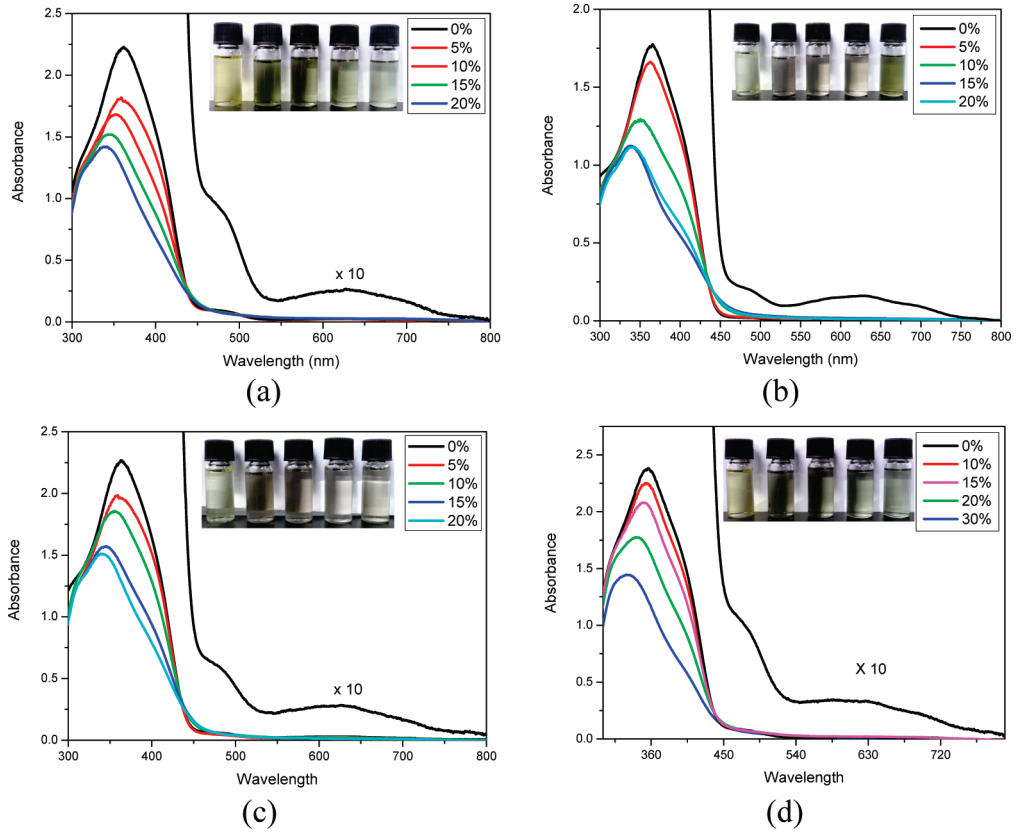

Figure 3. UV−vis spectra of **P1** (a) (6.32×10^{-5} M), (b) **P2** (8.64×10^{-5} M), (c) **P3** (5.86×10^{-5} M), and (d) **P4** (6.58×10^{-5} M) upon addition of TFA. (Inset: from left to right, **P1**−**4** in 0%, 5%, 10%, 15% and 20% TFA/THF, v/v.)

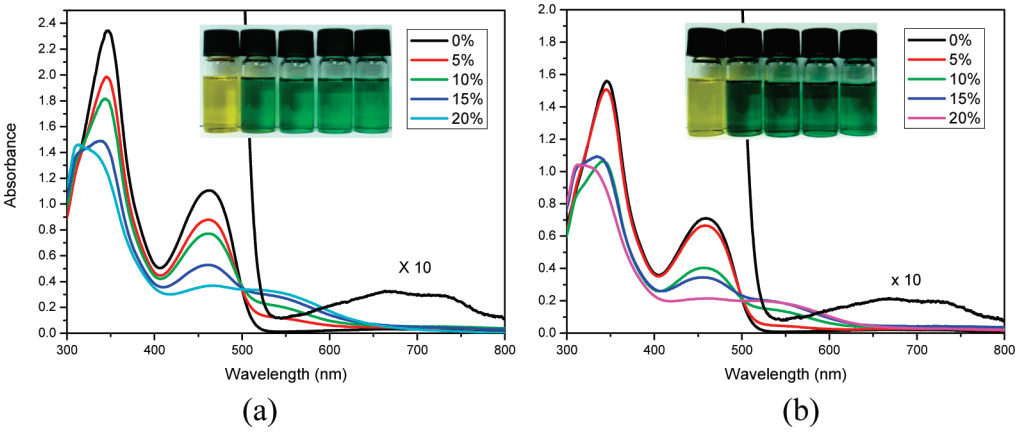

Figure 4. UV−vis spectral and color changes of (a) **P5** (3×10^{-5} M) (inset: from left to right, **P5** in 0%, 5%, 10%, 15% and 20% TFA/THF, v/v), and (b) **P6** (2.09×10^{-5} M) (inset: from left to right, **P6** in 0%, 5%, 10%, 15% and 20% TFA/THF, v/v), upon addition of TFA in THF.

addition of TFA, a new band at 533 nm was developed, which was ascribed to the formation of the azulenium cation.

The color changes of **M1** and **M2** and **P1**−**P6** upon the addition of TFA were also monitored. In contrast to the beautiful blue color of azulene, **M1** was almost colorless, while **M2** and polymers **P1**−**P6** were yellow or yellowish-green in THF. Upon the addition of TFA, **M1** gradually produced a color change from colorless to reddish brown (Figure 2a, insert). The color of protonated **M2** varied more sensitively than **M1** with the concentration of TFA, the color of **M2** in THF changed from yellow to light pink, pink, blue and finally purple when the concentration of TFA increased from 0% to 20% (Figure 2b, insert). However, polymers **P1**−**P4** showed small color changes from pale yellow to light brown, which was consistent with the changes in the UV region in their respective UV−vis spectra in the presence of TFA. In contrast, polymers **P5** and **P6** changed from orange to green upon the addition of TFA (Figure 3, insert). Moreover, neutralization of acidic solutions of **M1** and **M2** and polymers **P1**−**P6** with triethylamine did not lead to recovery of the initial color, indicating that protonation at the 1 or 3 positions of azulene is not reversible. Irreversibility of the protonation of **M1**, **M2**, and **P1**−**P6** is probably due to the oxidation or decomposition of protonated azulene species under acidic condition.

Table 2. Optical Properties of M1 and M2 and P1−P6

	UV−vis[a]				fluorescence (nm)[b]		
code	λ_{max} (nm)	Solvent	λ_{max} (nm)	solvent[d]	λ_{max}(nm)	solvent	ϕ_f
M1	331(58700), 392(14400),[c] 630 (380)	THF	311	THF/TFA (7: 3)	386	THF/TFA(7: 3)	0.02
M2	341(35600), 449 (11800), 654 (300)	THF	308, 508	THF/TFA(8: 2)	440	THF/TFA(8: 2)	0.06
P1	362 (35200), 477 (1500),[c] 630 (400)	THF	339	THF/TFA(8: 2)	n.a.[e]	THF/TFA(8: 2)	0
P2	363(20500), 480(240),[c] 629(190)	THF	340	THF/TFA(8: 2)	n.a.[e]	THF/TFA(8: 2)	0
P3	364 (38700), 478(1040),[c] 630 (460)	THF	341	THF/TFA(8: 2)	n.a.[e]	THF/TFA(8: 2)	0
P4	355 (36100), 477 (1210),[c] 630 (200)	THF	343	THF/TFA(7: 3)	n.a.[e]	THF/TFA(7: 3)	0
P5	347 (78100), 464 (36900), 670 (1070), 727 (970)	THF	313, 464, 533	THF/TFA(8: 2)	385	THF/TFA(8: 2)	0.004
P6	346 (74500), 460 (33900), 669 (1010), 724 (930)	THF	314, 455, 533	THF/TFA(7: 3)	385	THF/TFA(7: 3)	0.01

[a] The values in the parentheses are molar absorptivitives (ε) with units of L $mol^{-1}cm^{-1}$. [b] The fluorescence efficiencies (ϕ_f) of the model compounds **M1** and **M2** and polymers **P5** and **P6** in THF/TFA were measured by using quinine sulfate (1.0×10^{-5} M solution in 0.1 M H_2SO_4, assuming ϕ_f of 0.55 as a standard. λ_{ex} (excitation wavelength) = 316 and 378 nm for **M1** and **M2**, respectively; λ_{ex} = 295 nm for **P5** and **P6**. [c] sh = shoulder peak. [d] THF/TFA = volume to volume. [e] n.a. = not applicable.

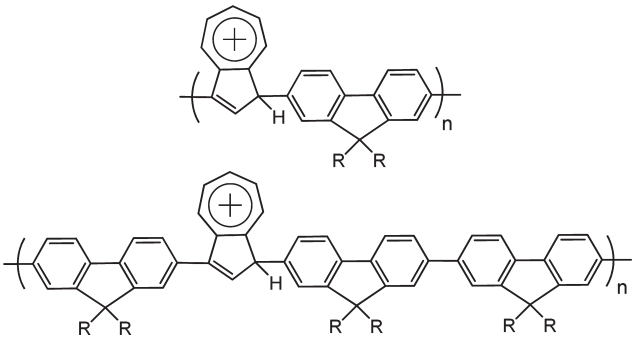

In comparison to colorless naphthalene, the blue color of azulene is due to a weak repulsive energy between the two electrons in the nearly orthogonal highest occupied molecular orbital (HOMO) and lowest unoccupied molecular orbital (LUMO) orbitals. Substitution at either the 1 or 3 position of the parent azulene ring has a strong effect on the electronic structure and photophysical properties of azulene derivatives.[42] Thus, the color change closely relates to the perturbation of the molecular orbitals of the azulene moiety, which could be induced by substitution/protonation. The azulene ring resembles an electron-rich five-membered pyrrole ring, which can undergo electrophilic substitution reactions at the 1 and 3 positions. Therefore, the addition of TFA leads to the formation of poly(azulenium cation)s, resulting in the electronic spectral and color changes.

Fluorescence Spectroscopic Study. The fluorescence spectra of polymers **P1**−**P6** and model compounds **M1** and **M2** were determined and they were found to be nonfluorescent in the absence of TFA in various organic solvents such as THF, $CHCl_3$, acetonitrile, toluene, etc. Upon the addition of TFA, **M1** and **M2** gave light with λ_{max} at 386 and 440 nm respectively (Figure 5a and b). Polymers **P1**−**P4** gave no fluorescence even in acidic THF solution. On the contrary, **P5** and **P6** emitted fluorescence with a λ_{max} of 385 nm (Figure 5c,d). Similar to the absorption spectra, the intensity of fluorescence of **M1** and **M2** and **P5** and **P6** varied with the concentration of TFA. For example, the fluorescence intensity of **M2** reached to the highest level when the concentration of TFA was 15%. A further increase in the TFA concentration (20%, v/v), however, resulted in a drop in the intensity of the fluorescence. The relative fluorescence efficiencies (ϕ_f) of **M1** and **M2** and polymers **P5** and **P6** in THF were measured by using quinine sulfate as a standard. The ϕ_fs of **M1** and **M2** were 0.02 and 0.06 in THF/TFA (v/v = 80/20), being larger by 20,000 and 60,000 times, respectively, than the ϕ_f value of the parent azulene (ϕ_f of S_1-S_0: 10^{-6}).[26] The ϕ_f values of polymers **P5** and **P6** (ϕ_f: 0.004 and 0.01, respectively) were relatively smaller than the two model compounds **M1** and **M2**. This is because strong self-absorption (absorption and fluorescence band overlap) results in a reduction in the fluorescence quantum yield. Another plausible reason is likely due to the presence of nonprotonated azulene units in the polymer backbone, thus reducing the fluorescence intensity.

In order to gain insight into the effect of the formation of tropylium ions on the emission of azulene−fluorene oligomers and polymers, density functional theory (DFT) calculations using two compounds **M1** and **M2** were performed. The HOMO and LUMO of **M1** and **M2** in the neutral and protonated state were estimated by DFT. The DFT calculations found that the azulene ring dominates the LUMO, whereas the fluorene moiety mainly contributes to HOMO. The anomalous fluorescence of azulene emission from S_2 instead of S_1 was due to the extraordinarily large energy gap of S_1-S_2, which was responsible for the emission of azulene from S_2 state. Protonation of azulene and the subsequent formation of azulenium cations lead to the remarkable changes in the S_1 and S_2 energy levels, as well as the HOMO−LUMO gap. As a result, its photophysical properties were expected to be altered accordingly. The band gap (E_g) of **M1-H**$^+$ and **M2-H**$^+$ were 0.561 and 0.594 eV, respectively, which were much lower than corresponding values (1.679 and 1.641 eV) of neutral **M1** and **M2**, respectively. The reduction in E_g could be attributed to two factors: (1) the formation of aromatic tropylium cation, and (2) the loss of aromaticity of the five-membered ring. Compared to the relatively large energy difference of S_1 (LUMO) and S_2 (LUMO+1), which is responsible for the spectral abnormality of azulene, **M1-H**$^+$ and **M2-H**$^+$ exhibited lower values of $\Delta E_{S1\text{-}S2}$ than **M1** and **M2** by 0.56 and 0.44 eV, respectively. Therefore, the HOMO and LUMO changes in the protonated **M1** and **M2** and **P5** and **P6** are believed to be attributed to the "switching on" of the fluorescence. However, the reasons for the absence of fluorescence in **P1**−**P4** upon the addition of TFA are unclear.

Spectroelectrochemical Behavior and Electrochromic Device. The cyclic voltammetric (CV) data and HOMO and LUMO values for polymers **P1**−**P6** and two model compounds **M1** and **M2** are summarized in Table 3. Two typical cyclic voltammograms of polymers **P3** and **P5** are shown in Figure 6. Polymers **P1**−**P6** revealed one irreversible oxidation redox wave in the range 0.97−1.09 V under an anodic sweep. The electron removal for polymer **P3** or **P5** occurs at the electron-rich cyclopentadiene part of the azulene ring to form a cationic radical, which probably further rearranges to form a closed shell structure (Scheme 3). The formation of similar tropylium cation radicals for azulene and its derivatives have been identified by electron spin resonance spectroscopy in the literatures.[43,44] The energy levels of the

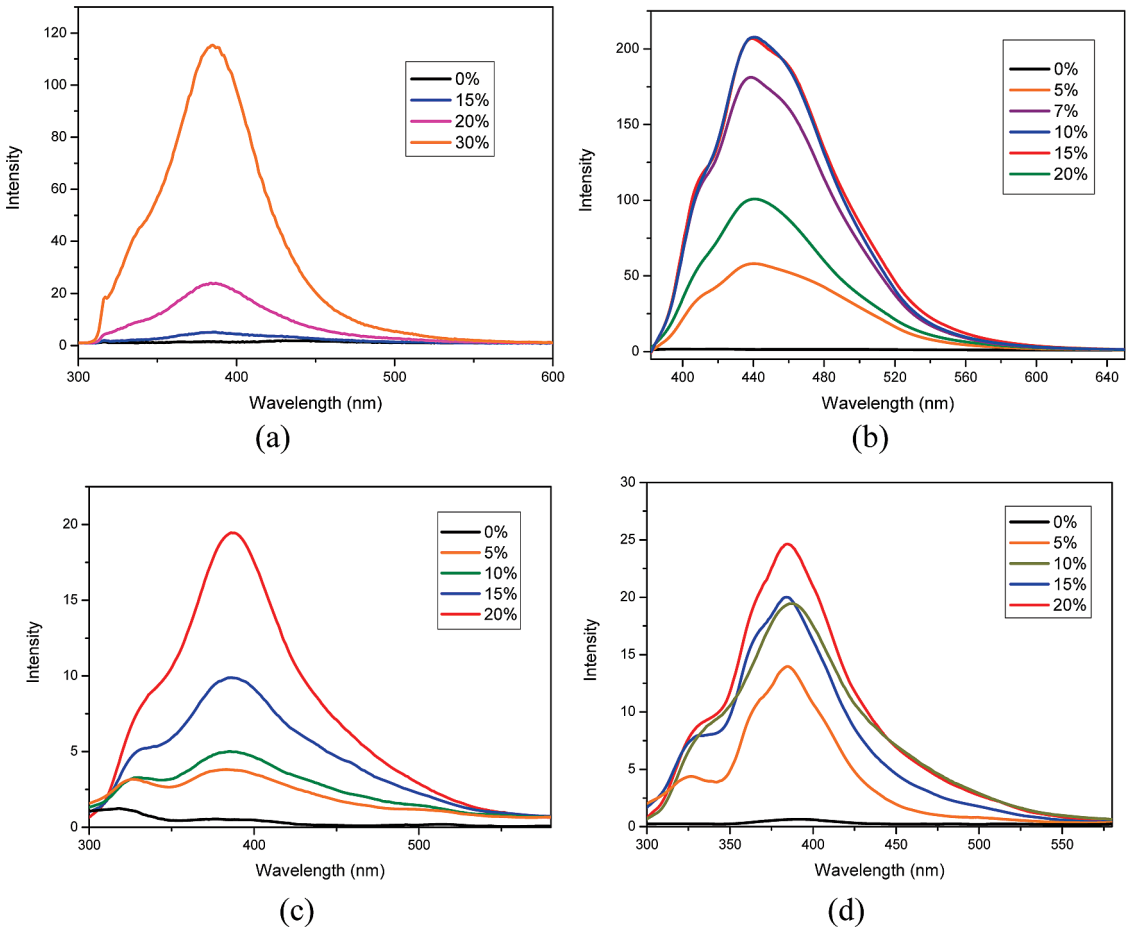

Figure 5. Fluorescence spectra of (a) **M1** (3.53×10^{-5} M), (b) **M2** (2.34×10^{-5}), (c) **P5** (3.00×10^{-5}), and (d) **P6** (2.09×10^{-5}) in the presence of TFA. The excited wavelengths (λ_{ex}) are 316, 378, 295, 295 nm, for **M1**, **M2**, **P5**, and **P6**, respectively.

Table 3. Electrochemical Properties of M1 and M2 and P1−P6

	oxidation potential (vs. Ag/AgCl)					
code	$E_{1/2}$ (V)	$E_{p,a}$ (V)[d]	abs λ_{onset} (nm)	E_g (eV)[a]	HOMO[b] (eV)	LUMO[c] (eV)
M1	0.80	0.89	780	1.59	5.16	3.57
M2	0.83	1.03	788	1.57	5.19	3.62
P1	0.88	1.02	765	1.62	5.24	3.62
P2	0.93	1.09	764	1.62	5.29	3.67
P3	0.94	1.08	769	1.61	5.30	3.69
P4	0.86	0.97	776	1.60	5.33	3.73
P5	0.84	0.99	784	1.58	5.20	3.62
P6	0.88	1.00	791	1.57	5.24	3.67

[a] The data were calculated by the equation: $E_g = 1240/\text{Abs}\,\lambda_{onset}$. [b] The HOMO energy levels were calculated from cyclic voltammetry and were referenced to ferrocene (4.8 eV). [c] LUMO = HOMO − E_g. [d] Anodic peak potential ($E_{p,a}$).

HOMO and LUMO of the polymers were estimated from the oxidation onset (E_{onset}) and the onset absorption wavelength of the UV−vis spectra, and the results are given in Table 3. The introduction of azulene in conjugated polymers leads to a substantial reduction in oxidation of potentials. For example, polymer **P5** has a lower anodic oxidation peak potential ($E_{p.a}$ = +0.99 V vs Ag/AgCl) than homopolymer poly(9,9-dihexylfluorene) ($E_{p.a}$ = +1.59 V[45] vs Ag/AgCl). Similarly, the E_g values of the model compounds and polymers were considerably decreased compared with that of homopolymer poly(9,9-dihexylfluorene). The E_g values of the polymers was reduced from 2.86 eV[45] for poly(9,9-dihexylfluorene) to around 1.60 eV for the copolymers of fluorene and azulene, revealing that the inclusion of azulene in the polymer backbone can significantly lower the E_g of conjugated polymers.

Scheme 3. Oxidation Pathway of Polymers P1−P4

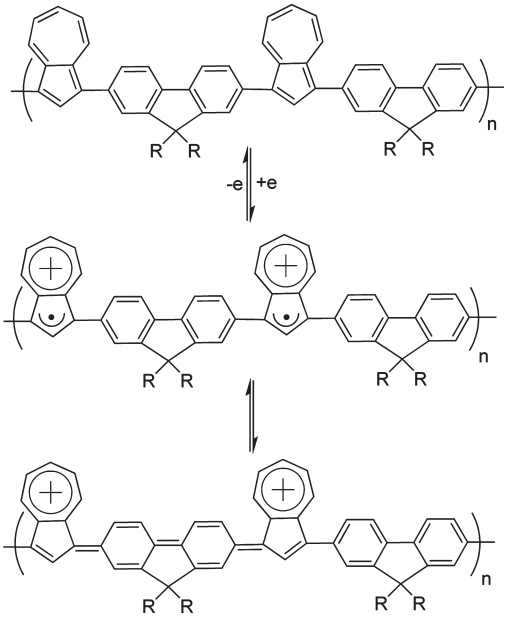

Electrochromic devices with a sandwich structure of PET-ITO/electrochromic polymer/gel polyelectrolyte/PET-ITO

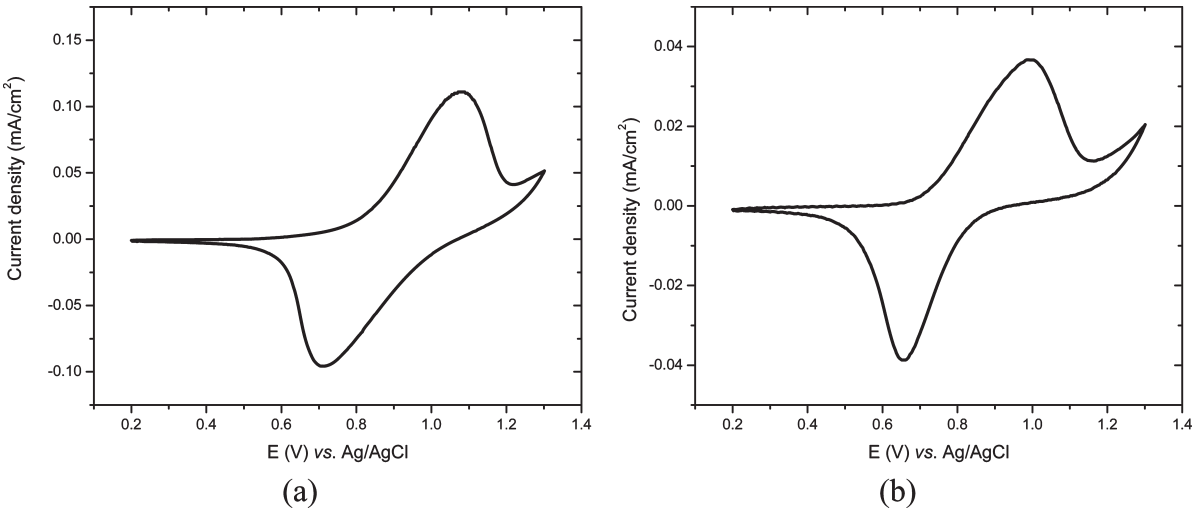

Figure 6. Cyclic voltammograms of (a) **P3**, and (b) **P5** on ITO-coated glass substrate in 0.1 M $LiClO_4$/acetonitrile at a scan rate of 25 mV/s.

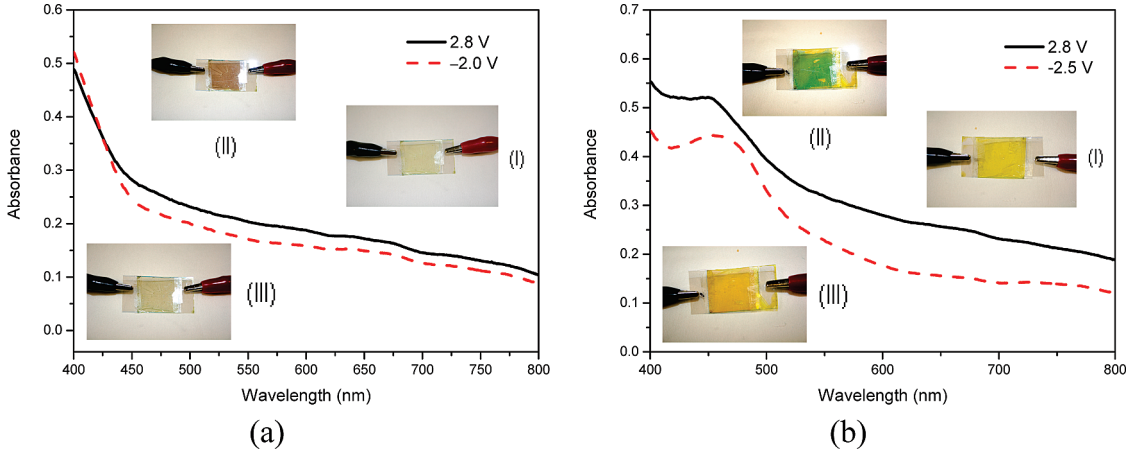

Figure 7. UV−vis spectra of (a) PET-ITO/**P3**/PMMA-PC-$LiClO_4$/PET-ITO device and (b) PET-ITO/**P5**/PMMA-PC-$LiClO_4$/PET-ITO device. The insets show the color switches of spin-coated films: (I) neutral and unswitched; (II) electrochemically oxidized; (III) neutral after electrochemical switching.

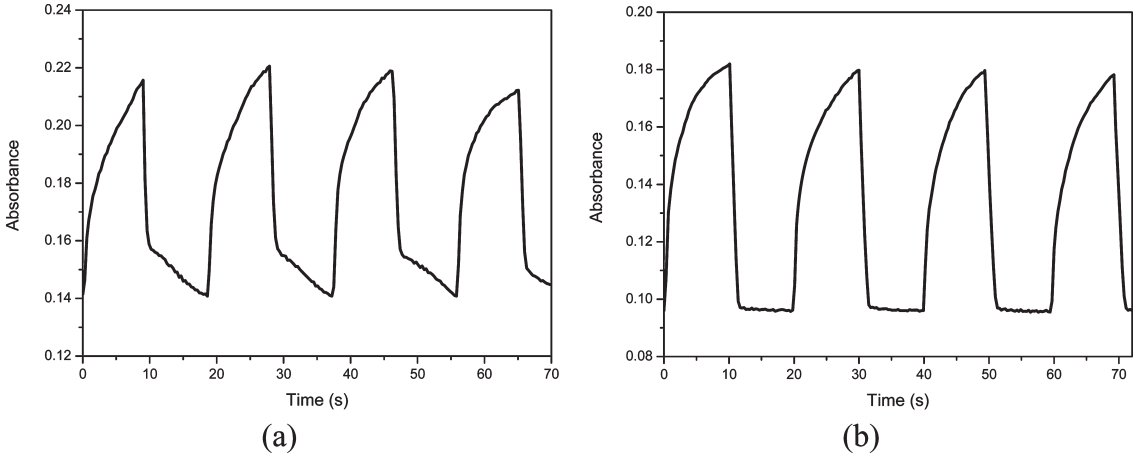

Figure 8. Absorbance−time profiles of (a) PET-ITO/**P3**/PMMA-PC-$LiClO_4$/PET-ITO device at 540 nm and (b) PET-ITO/**P5**/PMMA-PC-$LiClO_4$/PET-ITO device at 630 nm.

were fabricated. Spectroelectrochemical analysis of **P3** and **P5** films was carried out on an ITO-coated glass substrate, and electrochromic behavior was examined when the applied potential was changed. The color of polymer **P3** was changed from pale yellowish-green at 0 and −2.0 V at the initial state and electrochemical reduced state to light brown at +2.8 V at the electrochemical oxidized state. In contrast, the color of **P5** changed from yellow at the initial state and electrochemical reduced state to green at the electrochemical oxidized state. Two typical CVs are shown in Figure 7. When the

applied potential was increased positively from −2.5 to +2.8 V, the characteristic absorbance peak of the **P5** film shifted from 462 to 452 nm, which is approximately close to the absorption λ_{max} value in THF (464 nm). However, no apparent peak for **P3** was observed because its absorption λ_{max} is located in the UV zone.

The response time upon electrochromic switching of the polymer film between its reduced and oxidized forms was monitored (Figure 8). The color switching time, which is defined as the time required for 95% of the full change in absorbance after switching potential, was estimated by applying a potential step. Thin films of polymer **P3** would require 8.1 s for switching absorbance at 540 nm and 6.8 s for bleaching. In contrast, thin film **P5** would require about 8.6 s for coloration at 630 nm and 1.3 s for bleaching. It likely suggests that the introduction of more fluorene units in the polymer backbone would lead to the reduction in the bleaching time.

Conclusions

Azulene-fluorene conjugated polymers **P1**−**P6** and model compounds **M1** and **M2** were synthesized from 1,3-dibromoazulene or 1,3-bis(7-bromo-9,9-dihexylfluoren-2-yl)azulene and the suitable mono or diborate through Suzuki cross coupling reactions. Being different from other fluorene conjugated copolymers, all of the polymers studied in this paper were nonfluorescent due to the presence of azulene moieties which made the polymers' fluorescence silent. However, upon the addition of TFA to THF solutions, **P5** and **P6** and **M1**−**2** became fluorescent with emission λ_{max} values from 385 to 440 nm and relative quantum yields of 0.004−0.06. The formation of poly(azulenium cation)s in those polymers, which alter the unusual electronic characteristics of azulene, has an effect on activating the fluorescence of the polymers. **P5** and **P6** and **M1** and **M2** were found to show the significant color changes upon the addition of TFA in THF. **P1**−**P6** had low band gaps (1.57−1.62 V), which were lower than that of poly(3-hexylthiophene) (1.9−2.0 eV),[46] suggesting that the azulene-containing conjugated polymers have potential in other applications of organic electronic materials such as field effect transistors. Electrochromic devices with a sandwich structure of PET-ITO/electrochromic polymer/gel polyelectrolyte/PET-ITO were fabricated and color changes of the polymer films have been demonstrated. The fluorene-azulene conjugated polymers offer an opportunity in the application of pH-sensing and electrochromic materials, etc. Integration of proper alternative comonomers, such as, dialkoxythienyl units, into azulene-based electrochromic conjugated copolymers would play a synergistic role in improving the device properties such as stability, response time and contrast and desired colors. These types of electrochromic polymers are currently under the investigation in our laboratory.

Acknowledgment. The authors would like to thank the Agency for Science, Technology and Research (A*STAR) for financial support.

References and Notes

(1) (a) Lash, T. D.; El-Beck, J. A.; Ferrence, G. M. *J. Org. Chem.* **2007**, *72*, 8402–8415. (b) El-Beck, J. A.; Lash, T. D. *Eur. J. Org. Chem.* **2007**, 3981–3990.
(2) Lash, T. D.; Colby, D. A.; Graham, S. R.; Chaney, S. T. *J. Org. Chem.* **2004**, *69*, 8851–8864.
(3) Wakabayashi, S.; Kato, Y.; Mochizuki, K.; Suzuki, R.; Matsumoto, M.; Sugihara, Y.; Shimizu, M. *J. Org. Chem.* **2007**, *72*, 744–749.
(4) Amatatsu, Y. *J. Phys. Chem. A* **2007**, *111*, 5327–5332.
(5) Mollerstedt, H.; Piqueras, M. C.; Crespo, R.; Ottosson, H. *J. Am. Chem. Soc.* **2004**, *126*, 13938–13939.
(6) Bearpark, M. J.; Bernardi, F.; Clifford, S.; Olivucci, M.; Robb, M. A.; Smith, B. R.; Vreven, T. *J. Am. Chem. Soc.* **1996**, *118*, 169–175.
(7) (a) Gordon, M. *Chem. Rev.* **1952**, *50*, 127–200. (b) Beer, M.; Longuet-Higgins, H. C. *J. Chem. Phys.* **1955**, *23*, 1390–1391. (c) Anderson, A. G.Jr.; Steckler, B. M. *J. Am. Chem. Soc.* **1959**, *81*, 4941–4946. (d) Rentzepis, P. M. *Chem. Phys. Lett.* **1969**, *3*, 717–720. (e) Murata, S.; Iwanaga, C.; Toda, T.; Kokubun, H. *Chem. Phys. Lett.* **1972**, *3*, 101–104.
(8) (a) Strachota, A.; Cimrova, V.; Thorn-Csanyi, E. *Macromol. Symp.* **2008**, *268*, 66–71. (b) Peart, P. A.; Repka, L. M.; Tovar, J. D. *Eur. J. Org. Chem.* **2008**, 2193–2206.
(9) Shoji, T.; Ito, S.; Toyota, K.; Yasunami, M.; Morita, N. *Chem.—Eur. J.* **2008**, *14*, 8398–8408.
(10) (a) Ito, S.; Kubo, T.; Morita, N.; Ikoma, T.; Tero-Kubota, S.; Kawakami, J.; Tajiri, A. *J. Org. Chem.* **2005**, *70*, 2285–2293. (b) Ito, S.; Kubo, T.; Morita, N.; Ikoma, T.; Tero-Kubota, S.; Tajiri, A. *J. Org. Chem.* **2003**, *68*, 9753–9762.
(11) Colby, D. A.; Ferrence, G. M.; Lash, T. D. *Angew. Chem., Int. Ed.* **2004**, *43*, 1346–1349.
(12) Ito, S.; Inabe, H.; Morita, N.; Ohta, K.; Kitamura, T.; Imafuku, K. *J. Am. Chem. Soc.* **2003**, *125*, 1669–1680.
(13) (a) Estdale, S. E.; Brettle, R.; Dummur, D. A.; Marson, C. M. *J. Mater. Chem.* **1997**, *7*, 391–401. (b) Hussain, Z.; Hopf, H.; Pohl, L.; Oeser, T.; Fischer, A. K.; Jones, P. G. *Eur. J. Org. Chem.* **2006**, 5555–5569.
(14) Wang, F.; Lai, Y.-H. *Macromolecules* **2003**, *36*, 536–538.
(15) Wang, F.; Lai, Y.-H.; Han, M.-Y. *Macromolecules* **2004**, *37*, 3222–3230.
(16) Porsch, M.; Sigl-Seifert, G.; Daub, J. *Adv. Mater.* **1997**, *9*, 635–639.
(17) Mrozek, T.; Gorner, H.; Daub, J. *Chem.—Eur. J.* **2001**, *7*, 1028–1040.
(18) Zielinski, T.; Kedziorek, M.; Jurczak, J. *Tetrahedron Lett.* **2005**, *46*, 6231–6234.
(19) Salman, H.; Abraham, Y.; Tal, S.; Meltzman, S.; Kapon, M.; Tessler, N.; Speiser, S.; Eichen, Y. *Eur. J. Org. Chem.* **2005**, 2207–2212.
(20) Zielhisk, T.; Kedziorek, M.; Jurczak, J. *Chem.—Eur. J.* **2008**, 838–846.
(21) Lambert, C.; Noell, G.; Zabel, M.; Hampel, F.; Schmaelzlin, E.; Braeuchle, C.; Meerholz, K. *Chem.—Eur. J.* **2003**, *9*, 4232–4239.
(22) Cristian, L.; Sasaki, I.; Lacroix, P. G.; Donnadieu, B.; Asselberghs, I.; Clays, K.; Razus, A. C. *Chem. Mater.* **2004**, *16*, 3543–3551.
(23) Kihara, N.; Nakayama, H.; Fukutomi, T. *Macromolecules* **1997**, *30*, 6385–6387.
(24) Wang, F.; Lai, Y.-H.; Kocherginsky, N. M.; Kosteski, Y. Y. *Org. Lett.* **2003**, *5*, 995–998.
(25) Wang, F.; Lai, Y.-H.; Han, M. *Org. Lett.* **2003**, *5*, 4791–4794.
(26) Rentzepis, P. M. *Chem. Phys. Lett.* **1969**, *3*, 717–720.
(27) Bearpark, B. R.; Vreven, T. *J. Am. Chem. Soc.* **1996**, *118*, 169–175.
(28) Sprutta, N.; Siczek, M.; Latos-Grazynski, L.; Pawlicki, M.; Szterenberg, L.; Lis, T. *J. Org. Chem.* **2007**, *72*, 9501–9509.
(29) Ito, S.; Ando, M.; Nomura, A.; Morita, N.; Kabuto, C.; Mukai, H.; Ohta, K.; Kawakami, J.; Yoshizawa, A.; Tajiri, A. *J. Org. Chem.* **2005**, *70*, 3939–3949.
(30) Ito, S.; Nomura, A.; Morita, N.; Kabuto, C.; Kobayashi, H.; Maejima, S.; Fujimori, K.; Yasunami, M. *J. Org. Chem.* **2002**, *67*, 7295–7302.
(31) Shunji, I.; Shigeru, K.; Tetsuo, O.; Noboru, M.; Toyonobu, A. *J. Org. Chem.* **2001**, *66*, 2470–2479.
(32) Jonsson, L. *Acta Chem. Scand.* **1981**, *B 35*, 683–689.
(33) Waltman, R. J.; Bargon, J. *Can. J. Chem.* **1986**, *64*, 76–95.
(34) Neikam, W. C.; Desmond, M. M. *J. Am. Chem. Soc.* **1964**, *86*, 4811–4814.
(35) Jia, P.; Xu, J.; Ma, J.; Lu, X. *Eur. Polym. J.* **2009**, *45*, 772–778.
(36) Schwendeman, I.; Hwang, J.; Welsh, D. M.; Tanner, D. B.; Reynolds, J. R. *Adv. Mater.* **2001**, *13*, 634–637.
(37) Sonmez, G.; Meng, H.; Wudl, F. *Chem. Mater.* **2004**, *16*, 574 580.
(38) Beaupre, S.; Dumas, J.; Leclerc, M. *Chem. Mater.* **2006**, *18*, 4011–4018.
(39) Anderson, A. G.; Nelson, J. A.; Tazuma, J. J. *J. Am. Chem. Soc.* **1953**, *75*, 4980–4989.
(40) Plattner, P. A.; Heilbronner, E.; Weber, S. *Helv. Chim. Acta* **1952**, *35*, 1036–1039.

(41) Oda, M.; Fukuta, A.; Kajioka, T.; Uchiyama, T.; Kainuma, H.; Miyatake, R.; Kuroda, S. *Tetrahedron* **2000**, *56*, 9917–9925.
(42) Liu, R. S. H.; Muthyala, R. S.; Wang, X.-S.; Asato, A. E.; Wang, P.; Ye, C. *Org. Lett.* **2000**, *2*, 269–271.
(43) Cooksey, C. J.; Courtneidge, J. L.; Davies, A. G.; Gregory, P. S.; Evans, J. C.; Rowlands, C. C. *J. Chem. Soc., Perkin Trans. 2* **1988**, 807.
(44) Fabian, G.; Markus, S.; Hans-Juergen, H.; Peter, U. *J. Chem. Soc., Perkin Trans. 2: Phys. Org. Chem.* **1995**, *2*, 215–220.
(45) Liu, B.; Yu, W.-L.; Lai, Y.-H.; Huang, W. *Chem. Mater.* **2001**, *13*, 1984–1991.
(46) Shrotriya, V.; Ouyang, J.; Tseng, R. J.; Li, G.; Yang, Y. *Chem. Phys. Lett.* **2005**, *411*, 138–143.